ChemComm

Check for updates

Amyloid-like Prep1 peptides exhibit reversible blue-green-red fluorescence *in vitro* and in living cells†

Alessandra Monti,‡[a] Chiara Bruckmann,‡[b] Francesco Blasi,[b] Menotti Ruvo,[a] Luigi Vitagliano [ID] *[a] and Nunzianna Doti [ID] *[a]

PREP1-based peptides form amyloid-like aggregates endowed with an intrinsic blue-green-red fluorescence with an unusual sharp maximum at 520 nm upon excitation with visible light under physiological conditions. The peptide PREP1[117-132], whose sequence does not contain aromatic residues, presents a pH-dependent and reversible fluorescence, in line with its structural transition from β-sheet rich aggregates to α-helix structures. These findings further demonstrate that the non-canonical fluorescence exhibited by amyloids is an articulated phenomenon.

Non-covalent interactions play crucial roles in protein/peptide functionality as they dictate folding and oligomerization. An overwhelming number of investigations carried out in the last three decades have demonstrated that non-covalent interactions may also generate abnormally β-sheet rich structured states, commonly denoted as amyloid-like assemblies, which are believed to be the causative agents of a remarkable number of neurodegenerative diseases.[1–4] The discovery that proteins and peptides present a high propensity to adopt these states has also been exploited to develop new biomaterials characterized by intriguing mechanical and spectroscopic properties.[5] Interestingly, independently of their natural or synthetic origin, amyloid-like peptides generally emit fluorescence with a maximum in the blue field upon excitation with near-UV radiation (~370 nm).[6–14] Although the physicochemical determinants of these spectroscopic properties remain quite elusive, it has been recently shown that these assemblies can also emit in the red and near-infrared region when excited with radiation with wavelengths in the range 600–670 nm.[15]

In this scenario, we have recently found that the human protein Pbx-regulating protein-1 (PREP1)[16–18] contains two

cytotoxic amyloidogenic fragments, spanning residues 117-132 and 297-311.[19] The synthetic peptides corresponding to these PREP1 portions (henceforth called PREP1[117-132] and PREP1[297-311]) present all the hallmarks commonly associated with amyloid-like assemblies.[19] We associated the presence of these potentially harmful regions with the unusual stability of the parent PREP1 protein,[19,20] which likely acts as a protective factor to avoid the formation of toxic species.[19] Intriguingly, the spectroscopic characterization of the amyloid-like forms of PREP1[117-132] and PREP1[297-311] in complex with Thioflavin T (ThT) indicated a significant red-shift of the fluorescence emission peak.[19] Indeed, upon excitation at 450 nm, we observed a fluorescence emission peaked at 500–540 nm that is some 20–40 nm red-shifted compared to the canonical emissions of amyloid-bound ThT (480–485 nm).[21] To gain insights into this peculiar behavior, we have analyzed the intrinsic fluorescence properties of peptides PREP1[117-132], PREP1[297-311] and some mutated variants (Table S1, ESI†). Using a freshly prepared solution of PREP1[117-132], we initially assessed its propensity to form β-sheet rich aggregates at neutral pH by circular dichroism (CD) (Fig. S1A, ESI†) and dynamic light scattering (Fig. S1B, ESI†). Indeed, in line with previous observations,[19] the peptide forms high molecular weight species that present a strong dichroic negative band at ~228–230 nm. Interestingly, these aggregates present an intrinsic fluorescence emission covering the wavelength interval 500–600 nm if excited at wavelengths within the range 400–480 nm. As shown in Fig. 1A, a solution of PREP1[117-132] buffered at pH 7.0, shows a sharp peak, whose maximum is centered at 520 nm independently of the excitation wavelength in the range 400–480 nm (Fig. 1A). This type of fluorescence is quite different from that commonly exhibited by amyloid-like assemblies.[15] Notably, the intensity of the peak raised upon increasing the excitation wavelength with a sigmoidal dependence (Fig. 1B). This observation is in line with the absorption spectrum associated with the fluorescence emission that shows a progressive increase in absorption, starting from 440 nm to 480 nm (Fig. S1C, ESI†). To validate these unexpected observations, we investigated the impact of some selected mutations on the supra-molecular peptide aggregation and, therefore, on its spectroscopic

[a] *Institute of Biostructures and Bioimaging (IBB)-CNR, Via Mezzocannone 16, Naples 80134, Italy. E-mail: luigi.vitagliano@cnr.it, nunzianna.doti@cnr.it*

[b] *IFOM, Foundation FIRC (Italian Foundation for Cancer Research), Institute of Molecular Oncology, Via Adamello, 16, Milan 20139, Italy*

† Electronic supplementary information (ESI) available. See DOI: 10.1039/d1cc01145f
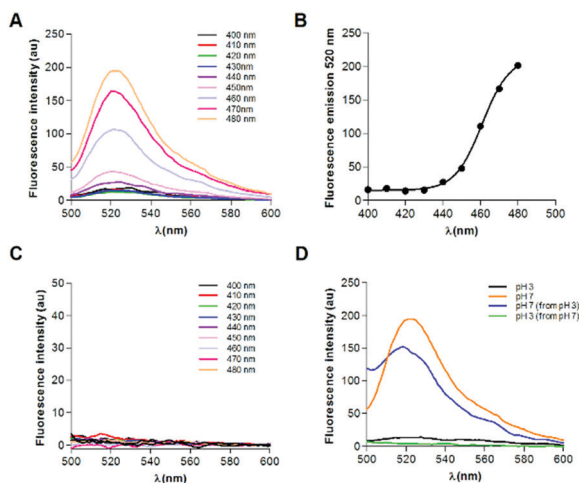
‡ These authors contributed equally to this work.

Fig. 1 The intrinsic fluorescence of PREP1[117-132] β-sheet rich aggregates. (A) Overlay of intrinsic fluorescence spectra of PREP1[117-132] in the 500–600 nm range upon excitation in the 400–480 nm range at pH 7.0. (B) Peptide fluorescence emission at 520 nm as a function of the excitation wavelengths. (C) Overlay of intrinsic fluorescence spectra of PREP1[117-132]$_{I122A,L125A,L129A,L132A}$ in the 500–600 nm range upon excitation in the 400–480 nm range at pH 7.0. (D) Overlay of intrinsic fluorescence spectra at pH 3.0, at pH 3.0 after pH 7.0 exposure and *vice versa*.

properties. This analysis was performed by collecting the fluorescence spectra of a previously reported mutated variant of PREP1 [117-132], PREP1[117-132]$_{I122A,L125A,L129A,L132A}$, in which the replacement of four hydrophobic residues with alanine induces the unfolding of the peptide, as shown by the CD spectrum (Fig. S1D, ESI†) and prevents aggregation.[19] As shown in Fig. 1C, PREP1 [117-132]$_{I122A,L125A,L129A,L132A}$ presents a radically different fluorescence profile compared to the parent peptide, as no emission is observed in the region 500–600 nm upon excitation in the 400–480 nm interval. Accordingly, this peptide does not absorb in the 400–480 nm interval (Fig. S1C, ESI†).

As PREP1[117-132] presents an intriguing pH-dependent reversible structural transition from β-sheet to α-helix when the pH is lowered at acidic values,[19] we monitored the peptide fluorescence as a function of the pH. We preliminary monitored the PREP1[117-132] structural transition and its reversibility. Indeed, we verified that the CD spectra at pH 3.0 obtained using freshly prepared peptide samples are similar to those obtained by lowering the pH from 7.0 to 3.0 and *vice versa*, despite the variation of the ionic strength associated with the pH lowering or increase (Fig. S1A and Methods, ESI†). As shown in Fig. 1D, the lowering of the pH from 7.0 to 3.0 abolished the fluorescence emission at 520 nm that was restored when the pH was brought from 3.0 to neutrality. Therefore, the data clearly show that the ability of PREP1 [117-132] to emit fluorescence radiation at physiological pH is reversibly switched off and on by changing the pH of the solution in line with the pH-dependent α-helix/β-sheet rich structural transitions exhibited by this peptide.

We then evaluated the ability of PREP1[117-132] to also emit the fluorescence in the near UV/blue and in the near-infrared regions that is generally exhibited by amyloid-like peptides.[15]

We therefore evaluated the PREP1[117-132] emission upon excitation at 370 and 670 nm. The emission spectrum of the peptide upon excitation at 370 nm showed two bands in the UV/ blue region, peaking at ∼420 and 450 nm (Fig. S2A, ESI†). A fluorescence signal centered at ∼710 nm was instead observed upon excitation at 670 nm (Fig. S2B, ESI†), in line with a recently discovered behavior of the amyloid-like assemblies.[15] It is worth mentioning that the emission at wavelengths >700 is not observed when the peptide is excited using radiation in the 400–480 nm range (Fig. S3, ESI†).

Due to the low solubility of the PREP1[297-311] peptide, its biophysical characterization was performed following its conjugation with a polyarginine (R8) stretch (R8PREP1[297-311]) (Table S1, ESI†). Preliminarily, we evaluated the effect of the R8 tag on the conformation of the peptide by CD analysis. Like the peptide without the R8,[19] at pH 7.0 R8PREP1[297-311] adopts a β-sheet rich state, showing a CD negative band at ∼228–230 nm (Fig. S4A, ESI†), thus demonstrating that the R8 moiety does not impact the conformational preferences of the peptide kept at pH conditions close to neutrality. However, unlike the parent peptide, which forms β-sheet rich assemblies in the entire 4.0–9.0 pH interval,[19] R8PREP1[297-311] assumes a random coil state at acidic pH as the CD spectrum presents a strong minimum at 198 nm (Fig. S4A, ESI†). In R8PREP1 [297-311], the formation of aggregated β-sheet rich assemblies at low pH values is likely prevented by the repulsive action exerted by the positively charged arginine side chains present in the tag. By studying the spectroscopic properties of the peptide R8PREP1[297-311], we observed that at pH 7.0 it shows a fluorescence emission peak at 520 nm upon excitation in the 440–480 nm range (Fig. 2A). On the contrary, no fluorescence was detected at pH 3.0 (Fig. S5A, ESI†), demonstrating the tight correlation between the structural and spectroscopic properties of these fragments. On this ground, we also evaluated the impact of the presence of the R8 stretch on the spectral properties of PREP1[117-132] and of its mutated variant PREP1 [117-132]$_{I122A,L125A,L129A,L132A}$. The R8-conjugates R8PREP1 [117-132] and R8PREP1[117-132]$_{I122A,L125A,L129A,L132A}$ were therefore synthesized and characterized (Table S1, ESI†). Somehow surprisingly, at acidic pH, the presence of the R8 tag in R8PREP1[117-132] prevents the formation of the helical state detected in PREP1[117-132], as shown by the CD analysis (Fig. S4B, ESI†). This observation may be explained by considering the perturbation caused by the R8 on the salt bridges that possibly
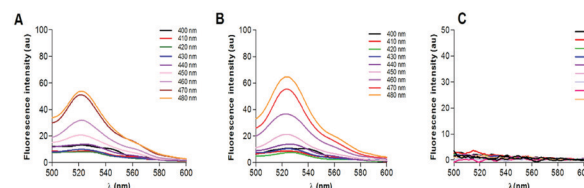

Fig. 2 Evidence for the intrinsic fluorescence of the R8PREP1[297-311]. Overlay of the intrinsic fluorescence spectra of R8PREP1[297-311] (A) R8PREP1[117-132] (B) and R8PREP1[117-132]I122A,L125A,L129A,L132A (C) upon excitation in the 400–480 nm range at pH 7.0.

stabilize the α-helix of the parent peptide.[22] On the contrary, the R8 tag did not impact the peptide structure at neutral pH (Fig. S4B, ESI†). The preservation of the β-sheet rich structure in R8PREP1[117-132] is reflected in the peptide fluorescence properties. Indeed, as shown in Fig. 2B, R8PREP1[117-132] presents a fluorescence emission in the 500–600 nm interval at pH 7.0, which is not detected for R8PREP1[117-132] at pH 3.0 (Fig. S5B, ESI†). As the untagged peptide, R8PREP1[117-132]$_{I122A,L125A,L129A,L132A}$ shows an unfolded conformation at both pH 3.0 and 7.0 (Fig. S4C, ESI†) and, accordingly, it does not show any intrinsic fluorescence at these conditions (Fig. 2C and Fig. S5C, ESI†).

We also investigated the intrinsic fluorescence emission of these peptides at the solid-state by performing confocal fluorescence microscopy analyses. Peptides were dissolved in hexafluoroisopropanol (HFIP) and allowed to dry on a glass surface at room temperature before analysis. Large aggregates of PREP1[117-132] are observed in bright-field microscopy without excitation (Fig. 3A). The same sample exhibits a remarkable fluorescence emission that peaked at 520 nm upon excitation at 488 nm (Fig. S6, ESI†). Moreover, confocal images of these dried samples showed that the peptide emitted in the blue, green and red fields following excitation at 405 nm (Fig. 3B), 488 and 555 nm (Fig. 3C and D), respectively. On the contrary, depositions of the non-aggregating peptide PREP1 [117-132]$_{I122A,L125A,L129A,L132A}$ performed under similar experimental conditions do not form fluorescent aggregates (Fig. S7, ESI†).

A similar but distinct behavior was exhibited by the aggregates formed by R8PREP1[117-132]. In this case, the red fluorescence was virtually absent (Fig. S8, ESI†), whereas the R8 variant of PREP1[297-311] showed an evident blue fluorescence with much weaker signals in the green and red fields (Fig. S9, ESI†).

The presence of the R8 stretch, which is generally used to facilitate the cellular uptake of peptides, provided us with the opportunity to evaluate the aggregation propensity of R8PREP1 [117-132] and R8PREP1[297-311] in living cells. In particular, we administered these peptides to a human lung epithelial cell line

Fig. 3 Intrinsic fluorescence of the solid aggregates of PREP1[117-132]. Bright-field (A) and fluorescent (B–D) confocal microscope images of a dried film of PREP1[117-132]. Fluorescent images were obtained by exciting in the UV spectral region of 4′,6-diamidino-2-phenylindole (DAPI) (405 nm) (B), the green fluorescent protein (GFP) (488 nm) (C) and the rhodamine (555 nm) (D). Scale bar: 90 μm.
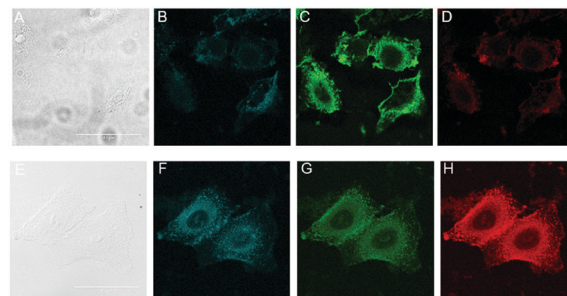

Fig. 4 Detection in cells of the fluorescence emitted by the aggregated peptide. Fixed-cell confocal microscopy images of A549 human lung epithelial cells treated with the peptide R8PREP1[117-132] (panels A–D) and R8PREP1[297-311] (panels E–H). Bright-field (A and E) and fluorescent (B–D and F–H) confocal microscope images of cells incubated with R8PREP1 peptides. Fluorescent images were obtained by exciting in the UV spectral region of 4′,6-diamidino-2-phenylindole (DAPI) (405 nm) (B), the green fluorescent protein (GFP) (488 nm) (C) and the rhodamine (555 nm) (D) after 8 h of incubation. Scale bar: 45 μm.

(A549) (at 5.0 μM in the culture medium). As shown in Fig. 4, a bright fluorescence is emitted in the blue, green and red fields for both peptides. The detected fluorescence was much higher than that observed at the solid-state (Fig. S8 and S9, ESI†). No fluorescence was detected when cells were treated with R8PREP1 [117-132]$_{I122A,L125A,L129A,L132A}$ (Fig. S10, ESI†).

The progressive characterizations of amyloid-like aggregates carried out in the last decades have unraveled unexpected and interesting properties that go well beyond their peculiar structural organization. A remarkable number of studies have shown that these assemblies, independently of their natural or synthetic origin, frequently present some spectroscopic properties whose underlying physicochemical determinants remain still quite elusive.[6–14] In particular, they can emit a blue fluorescence upon excitation with near-UV radiation (∼370 nm). Very recently, it has been shown that these assemblies are also able to emit at much higher wavelengths extending to the red and near-infrared region when excited with radiation with wavelengths in the range 600–670 nm.[15] We show here that the peptides PREP1[117-132] and R8PREP1[297-311], extracted from the sequence of the homeobox protein PREP1, in addition to these emissions, also present a strong fluorescence emission in the green region (maximum at 520 nm) upon excitation with visible light (wavelength 440–480 nm). Notably, when PREP1[117-132] is stained with the dye ThT,[19] the maximum emission is detected at 520 and not at 480 nm, the wavelengths typically observed for ThT.[21,23] This finding demonstrates that the intrinsic fluorescence of the peptide overcomes that produced by the amyloid-bound ThT. Interestingly, peptide fluorescence is observed in very different contexts, including buffered solution, solid-state, and living cells. Also, the green fluorescence exhibited by the peptide upon aggregation in living cells overlaps with that exhibited by the GFP protein[24] (Fig. S11, ESI†). Therefore, the design and interpretation of immunofluorescence experiments relying on green fluorescence impose caution when using peptides with a propensity to form amyloid-like aggregates to avoid misinterpretations.
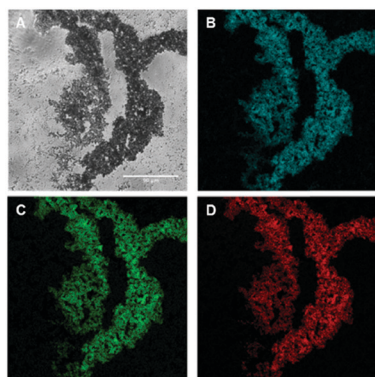
We have exploited the peculiar structural versatility of peptides, which can adopt different structural states, establishing a strict relationship between the β-sheet rich structure and the fluorescence emission. Indeed, we show that the reversible structural transition exhibited by PREP1[117-132] passing from neutral to acidic pH is an effective molecular switch to turn on and off the fluorescence emitted by the peptide. This finding is particularly intriguing considering the recent interest in reversible and non-reversible amyloids and their roles in functional or pathological processes.[25–27]

To the best of our knowledge, although fluorescence emissions with maxima in the region 480–500 nm have been reported for cyclic and/or aromatic oligopeptides upon temperature-induced aggregation,[28,29] the ability of soluble amyloid-like assemblies to absorb visible radiation and to emit green-red fluorescence, with a maximum at 520 nm, has been reported only for a phenylalanine-based peptide conjugated with a PEG moiety (PEG24-F6).[30] Worth noting, in the case of F6 adducts, the fluorescence could be only detected using a specific PEG conjugation, as similar F6 compounds containing other PEG moieties were not fluorescent in the green region.[30] It is also worth mentioning that the peptide PREP1[117-132] presents significant and distinctive features because it does not contain conjugated bonds nor aromatic and fluorescent residues (Tyr, Trp, and Phe). In this scenario, the present findings demonstrate that amyloid-like systems may exhibit other relevant spectroscopic properties in addition to the blue and the near-infrared fluorescence emission and that their fluorescence emission is an articulated process whose interpretation requires extensive efforts.

Conflicts of interest

There are no conflicts to declare.

Notes and references

1 I. Cherny and E. Gazit, *Angew. Chem., Int. Ed.*, 2008, **47**, 4062–4069.
2 F. Chiti and C. M. Dobson, *Annu. Rev. Biochem.*, 2017, **86**, 27–68.
3 J. Greenwald and R. Riek, *J. Mol. Biol.*, 2012, **421**, 417–426.
4 P. C. Ke, R. Zhou, L. C. Serpell, R. Riek, T. P. J. Knowles, H. A. Lashuel, E. Gazit, I. W. Hamley, T. P. Davis, M. Fandrich, D. E. Otzen, M. R. Chapman, C. M. Dobson, D. S. Eisenberg and R. Mezzenga, *Chem. Soc. Rev.*, 2020, **49**, 5473–5509.
5 G. Wei, Z. Su, N. P. Reynolds, P. Arosio, I. W. Hamley, E. Gazit and R. Mezzenga, *Chem. Soc. Rev.*, 2017, **46**, 4661–4708.
6 L. L. Del Mercato, P. P. Pompa, G. Maruccio, A. Della Torre, S. Sabella, A. M. Tamburro, R. Cingolani and R. Rinaldi, *Proc. Natl. Acad. Sci. U. S. A.*, 2007, **104**, 18019–18024.
7 M. Lu, C. F. Kaminski and G. S. K. Schierle, *Phys. Biol.*, 2020, **17**, 021001.
8 C. Diaferia, T. Sibillano, C. Giannini, V. Roviello, L. Vitagliano, G. Morelli and A. Accardo, *Chemistry*, 2017, **23**, 8741–8748.
9 D. Pinotsi, L. Grisanti, P. Mahou, R. Gebauer, C. F. Kaminski, A. Hassanali and G. S. Kaminski Schierle, *J. Am. Chem. Soc.*, 2016, **138**, 3046–3057.
10 F. T. Chan, G. S. Kaminski Schierle, J. R. Kumita, C. W. Bertoncini, C. M. Dobson and C. F. Kaminski, *Analyst*, 2013, **138**, 2156–2162.
11 C. Iannuzzi, M. Borriello, M. Portaccio, G. Irace and I. Sirangelo, *Int. J. Mol. Sci.*, 2017, **18**, 2551.
12 B. Apter, N. Lapshina, A. Handelman and G. Rosenman, *J. Pept. Sci.*, 2019, **25**, e3164.
13 L. Grisanti, M. Sapunar, A. Hassanali and N. Doslic, *J. Am. Chem. Soc.*, 2020, **142**, 18042–18049.
14 A. Shukla, S. Mukherjee, S. Sharma, V. Agrawal, K. V. Radha Kishan and P. Guptasarma, *Arch. Biochem. Biophys.*, 2004, **428**, 144–153.
15 J. Pansieri, V. Josserand, S. J. Lee, A. Rongier, D. Imbert, M. M. Sallanon, E. Kovari, T. G. Dane, C. Vendrely, O. Chaix-Pluchery, M. Guidetti, J. Vollaire, A. Fertin, Y. Usson, P. Rannou, J. L. Coll, C. Marquette and V. Forge, *Nat. Photonics*, 2019, **13**, 473–497.
16 F. Blasi, C. Bruckmann, D. Penkov and L. Dardaei, *BioEssays*, 2017, **39**, 1600245.
17 E. Longobardi, D. Penkov, D. Mateos, G. De Florian, M. Torres and F. Blasi, *Dev. Dyn.*, 2014, **243**, 59–75.
18 C. Bruckmann, S. Tamburri, V. De Lorenzi, N. Doti, A. Monti, L. Mathiasen, A. Cattaneo, M. Ruvo, A. Bachi and F. Blasi, *Sci. Rep.*, 2020, **10**, 16809.
19 N. Doti, A. Monti, C. Bruckmann, L. Calvanese, G. Smaldone, A. Caporale, L. Falcigno, G. D'Auria, F. Blasi, M. Ruvo and L. Vitagliano, *Int. J. Biol. Macromol.*, 2020, **163**, 618–629.
20 V. Lorenzo, F. Mascanzoni, L. Vitagliano, M. Ruvo and N. Doti, *Mol. Biotechnol.*, 2016, **58**, 328–339.
21 C. Xue, T. Y. Lin, D. Chang and Z. Guo, *R. Soc. Open Sci.*, 2017, **4**, 160696.
22 H. Lu, J. Wang, Y. Bai, J. W. Lang, S. Liu, Y. Lin and J. Cheng, *Nat. Commun.*, 2011, **2**, 206.
23 M. G. Di Carlo, V. Minicozzi, V. Fodera, V. Militello, V. Vetri, S. Morante and M. Leone, *Biophys. Chem.*, 2015, **206**, 1–11.
24 L. Yang, S. Nian, G. Zhang, E. Sharman, H. Miao, X. Zhang, X. Chen, Y. Luo and J. Jiang, *Sci. Rep.*, 2019, **9**, 11640.
25 R. Riek and D. S. Eisenberg, *Nature*, 2016, **539**, 227–235.
26 G. Cereghetti, S. Saad, R. Dechant and M. Peter, *Cell Cycle*, 2018, **17**, 1545–1558.
27 M. P. Hughes, M. R. Sawaya, D. R. Boyer, L. Goldschmidt, J. A. Rodriguez, D. Cascio, L. Chong, T. Gonen and D. S. Eisenberg, *Science*, 2018, **359**, 698–701.
28 A. Handelman, N. Kuritz, A. Natan and G. Rosenman, *Langmuir*, 2016, **32**, 2847–2862.
29 A. Handelman, N. Lapshina, B. Apter and G. Rosenman, *Adv. Mater.*, 2018, **30**, 1705776.
30 C. Diaferia, T. Sibillano, D. Altamura, V. Roviello, L. Vitagliano, C. Giannini, G. Morelli and A. Accardo, *Chemistry*, 2017, **23**, 14039–14048.